The Z-2018 emissions inventory of COS in Europe: A semiquantitative multi-data-streams evaluation

Sauveur Belviso, Isabelle Pison, Jean-Eudes Petit, Antoine Berchet, Marine Remaud, Leïla Simon, Michel Ramonet, Marc Delmotte, Victor Kazan, Camille Yver-Kwok, et al.

Atmospheric Environment 300 (2023) 119689

Contents lists available at ScienceDirect

Atmospheric Environment

journal homepage: www.elsevier.com/locate/atmosenv

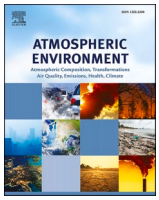

The Z-2018 emissions inventory of COS in Europe: A semiquantitative multi-data-streams evaluation

Sauveur Belviso *, Isabelle Pison, Jean-Eudes Petit, Antoine Berchet, Marine Remaud, Leïla Simon, Michel Ramonet, Marc Delmotte, Victor Kazan, Camille Yver-Kwok, Morgan Lopez

Laboratoire des Sciences du Climat et de l'Environnement, CEA-CNRS-UVSQ-Paris Saclay, UMR 8212, CE de Saclay, L'Orme des Merisiers, Bât 714, 91191, Gif-sur-Yvette, Cedex, France

HIGHLIGHTS

- We evaluate the European gridded anthropogenic emissions inventory of carbonyl sulfide (COS).
- The monitoring site of Gif-sur-Yvette (GIF, FR) has observations back to 2014.
- With GIF as end point, cluster analysis of winter air masses trajectories show that FR is not a net COS source.
- The existing inventory largely overestimates French COS emissions by about one order of magnitude.
- Perspectives are drawn as to the way this inventory should be revised.

ARTICLE INFO

Keywords:
Carbonyl sulfide
atmosphere
OCS
COS
anthropogenic emissions
HYSPLIT backtrajectories
cluster of air masses
inventory

ABSTRACT

The anthropogenic emissions of carbonyl sulfide (COS) and the uptake of this gas by terrestrial vegetation are major drivers of COS concentration variations in the atmosphere since the beginning of the industrial era. The fine spatial resolution (i.e., $0.1^\circ \times 0.1^\circ$) of the gridded anthropogenic emissions inventory of COS developed by Zumkehr et al. (2018), Z-2018 hereafter, is designed for a use by regional chemistry-transport models. In order to anticipate future applications at the regional scale, we carried out a first semiquantitative assessment of direct and indirect (i.e., from CS_2 conversion) COS anthropogenic emissions at the sub-country scale in France using historical governmental data. Better agreement between the two inventories was found for direct emissions of COS by coal power plants, than for indirect sources. The use in this latter case of a sub-country spatial scaling, based on industrial N_2O emissions, (1) strongly underestimates fluxes from food casings and cellulosic sponge industrial activities responsible for atmospheric CS_2 emissions in France, and (2) considerably overestimates emissions from Paris and surrounding areas, which are free of a rayon industry. A list of food casings and cellulosic sponge industrial sites is provided to produce a more realistic inventory of CS_2 sources in Europe. Nevertheless, a cluster analysis of wintertime air masses trajectories, with the atmospheric COS monitoring site of Gif-sur-Yvette (GIF) as end point, suggests that Z-2018 correctly identifies northern Germany and Belgium as sources of anthropogenic COS. In winter, when the wind blows from the NE sector, advection of anthropogenic COS from coal power plants is illustrated by synchronous variations in GIF and at the Trainou tall tower (distant of about 80 km) of a series of atmospheric pollution tracers, especially between COS and sulfates. These observations support the use of SO_2 emissions as temporal and sub-country spatial scaling factors of COS emissions by the coal industry.

1. Introduction

There is consensus as to the dominant role played by marine and anthropogenic sources on the one hand, and the plant sink on the other hand, in the global biogeochemical cycle of carbonyl sulfide (COS), which is the most abundant gaseous sulfur compound in the atmosphere

* Corresponding author.
E-mail address: sauveur.belviso@lsce.ipsl.fr (S. Belviso).

https://doi.org/10.1016/j.atmosenv.2023.119689
Received 23 September 2022; Received in revised form 18 January 2023; Accepted 28 February 2023
Available online 2 March 2023

(Whelan et al., 2018 and references therein). Our understanding of the historical variations of atmospheric COS, from preindustrial times to present, relies on a series of records of (1) air trapped in ice and firn over the long-term (e.g., Montzka et al., 2004; Aydin et al., 2008; Aydin et al., 2020), (2) ambient air collected around the globe from the year 2000 onward as part of the NOAA flask network (Montzka et al., 2007), and (3) total and partial COS columns retrieved from 1986 onward from ground-based remote sensing NDACC FTIR stations (Hannigan et al., 2022 and references therein). When combined, these records showed stability of COS concentrations in the preindustrial era up to 1850, a date from which COS rose exponentially up to the 1980s when the trend reversed (Campbell et al., 2017). By tracing the history of atmospheric COS mixing ratios using Monte Carlo simulations, Campbell et al. (2017) showed that the simulations were best able to replicate observations when a large industrial COS growth was combined with a large historical growth of the COS plant sink (i.e., +34% of growth) which was assumed to be proportional to the vegetation gross primary production (GPP). Since about 2016, almost all NOAA and NDACC stations show a decrease of COS in the free troposphere (https://gml.noaa.gov/hats/gases/OCS.html; Hannigan et al., 2022; Belviso et al., 2022a), a slowing of COS anthropogenic emissions likely being the cause of this tropospheric negative trend (Hannigan et al., 2022). However, an increasing uptake of COS by plants cannot be ruled out until a revised version of the 1980–2012 anthropogenic emissions budget of Zumkehr et al. (2018), hereafter named Z-2018, is made available for the 2013–2020 period. This gridded inventory encompasses 11 emission sectors (i.e., agricultural chemicals, aluminum, carbon black, industrial coal, residential coal, rayon staple, rayon yarn, industrial solvents, titanium dioxide, tires and pulp/paper industry) and has a $0.1^\circ \times 0.1^\circ$ spatial resolution. Biomass burning is not considered in the Z-2018 inventory. It employs a source spatial scaling procedure applied to country-level production or consumption yearly data. For example, country-level yearly rayon yarn production for year 2012 is converted into CS_2 emissions using an emission factor of 0.25 g CS_2 g^{-1} yarn, which is then spatially scaled at the sub-country level using industrial nitrous oxide (N_2O) emissions. In the case of industrial coal, country level coal consumption is first converted to carbon dioxide (CO_2) emissions; it is then converted to COS emissions using emission factors scaled by sulfur dioxide (SO_2) emissions to coal combustion (4.7–6.8 μmol COS mol CO_2^{-1}); finally this is spatially scaled at the sub-country level using energy industry and waste incinerator sulfur SO_2. According to Z-2018, the dominant source regions of atmospheric COS from anthropogenic activity, are, ranked by order of importance, China, Europe, USA & Canada and India. In all regions, except for USA & Canada, the viscose/rayon industries that make large use of carbon disulfide (CS_2), the major precursor of anthropogenic COS, are major indirect sources of COS (Zumkehr et al., 2018). Direct emission from coal combustion is ranked second. China's COS direct emissions from Z-2018 have been challenged by Yan et al. (2019). Those two inventories targeting China's COS direct emissions better agree on total emissions (Yan's estimates are 43% higher than those of Z-2018) than on their individual components, especially as to the relative contribution of coal combustion and aluminum production (Table 1).

COS and CS_2 anthropogenic emissions are inventoried in the North American (NA)-Pollutant Release and Transfer Register (PRTR) database (http://takingstock.cec.org/). Declarative cumulated emissions from USA & Canada for year 2012 (as combined direct and indirect COS emissions) were equal to 7.6 GgS yr^{-1}, to which an extra contribution from coal power plants not considered by the NA-PRTR should be added (i.e., 7.3 GgS yr^{-1}, where CO_2 data was collected from the Global Carbon Atlas, accessed September 2022, and converted to COS following Z-2018), whereas 35.2 GgS yr^{-1} were inventoried by Zumkehr et al. (2018). This difference, which exceeds a factor of 2, emphases the need to revise Z-2018 anthropogenic COS emissions in the USA and Canada too. Since 2012, the declared US and Canadian emissions have followed a decreasing trend of about 23% in 6 years. The overestimation of COS emissions in the USA and Canada in Z-2018 is qualitatively consistent with the last top-down assessment of the global COS budget of Remaud et al. (2022), who inferred a net global anthropogenic source approximately 20% lower than Z-2018. This decrease obtained by their global atmospheric inverse system was mainly driven by surface stations located over the USA.

Table 1
Assessment of two inventories targeting China's COS direct emissions.

	Anthropogenic COS direct emissions from China (GgS), year 2012	
	Zumkehr et al. (2018)	Yan et al. (2019)
Total direct emissions	93.6[a]	134[b]
Aluminum[c]	3.3	49[d]
Carbon black[c]	7.0	23[d]
Titanium dioxide[c]	15.6	14[d]
Total coal combustion[c]	64.1	11[d]

[a] Subtracting 91 GgS (indirect emissions by the rayon industry) from total emissions of 184.6 GgS
[b] Not considering the contribution from biomass burning (Yan's Fig. 1).
[c] Selected individual sources.
[d] Digitized from Figs. 1 and 2 in Yan et al. (2019).

Nevertheless, no qualitative/quantitative appraisals at the grid level of the Z-2018 anthropogenic emissions inventory for COS have been carried out so far. Here, we present a first assessment of the Z-2018 gridded inventory of direct/indirect emissions of COS for France and Western Europe, based on two complementary approaches. The first approach relies on the French facilities reporting an on-site release in the atmosphere of more than 50 tons per year either of CS_2 or of carbon dioxide (CO_2) produced from coal burning power plants. Atmospheric COS surveys, carried out downwind of the largest French anthropogenic CS_2 emission hotspot, also allowed us to assess the significance of viscose processors as direct sources of COS. The second approach uses Northern Hemispheric winter clusters of HYSPLIT back trajectories ending at the Gif-sur-Yvette COS monitoring site, as well as physico-chemical processes tracers collected semi-continuously in parallel with COS, to evaluate the reported hotspot locations stated in the Z-2018 inventory for Europe. Perspectives are then drawn as to the way this inventory should be revised.

2. Methods

2.1. The Z-2018 inventory of European anthropogenic sources of COS and French PRTR

The Z-2018 database is available publicly from the Campbell Lab Data Sharing facility (https://portal.nersc.gov/project/m2319/index.html). Masks of geographical regions were applied to estimate total and individual sector emissions for the year 2012 in Europe (EU27 + UK), selected European countries (including France), and two French sub-country levels: the city of Paris and Paris broader area (Ile-de-France, IDF). Moreover, data extractions were carried out at grid points and at the immediate proximity of French industrial plants reporting an on-site release to air of more than 50 tons per year either of CS_2 or of carbon dioxide (CO_2) produced from coal burning power plants. The "Registre des Rejets et des Transferts de Polluants (RRTP or IREP)" is the French inventory of potentially hazardous chemicals and/or pollutants released to air, water and soil (https://www.georisques.gouv.fr/donnees/bases-de-donnees/installations-industrielles-rejetant-des-polluants). Contrary to the Canadian, Mexican and U.S. online facilities tracking pollutant releases and transfers in North America (http://takingstock.cec.org/Query?Culture=en-US&IndustryLevel=3&Measure=3&MediaTypes=29&ReportType=1&ResultType=1&WatershedLevel=2), the list of IREP hazardous chemicals does not include COS. Neither COS nor CS_2 atmospheric emissions are taken into account by the European Environment Agency (https://industry.eea.europa.eu/pollutants/pollutant

-index). For this reason, the Z-2018 European gridded inventory of indirect production of COS from CS_2 could not be evaluated outside of France. Firstly, we extracted data from the IREP database and Z-2018 inventory; we then converted IREP's CS_2 and CO_2 declared emissions from food casings/cellulosic sponge manufacturers and coal power plants into COS emission, following Zumkehr et al. (2018).

2.2. *In situ* **observations**

2.2.1. *At Gif-sur-Yvette (GIF)*

Atmospheric COS mixing ratios were measured by gas chromatography (GC) at GIF (48.711 N, 2.147 E), at 7 m agl, from August 2014 to December 2021. The reader is referred to Belviso et al. (2016) and Belviso et al. (2020) for a description of GC COS measurements, their calibration and comparability with other atmospheric COS datasets. The GIF time series is presently made of 46,860 hourly data points available in Belviso et al. (2022a).

These data were collected in parallel with the atmospheric mixing ratios of CO_2 measured by Cavity Ring-Down Spectroscopy (CRDS, Picarro, Inc.), hydrogen (H_2, measured by GC), carbon monoxide (CO, measured by GC), ozone (O_3, measured by UV absorption), Radon-222 (^{222}Rn, measured with the active deposit method, that is, via the radioactive decay of its daughters attached to aerosols), particles less than 2.5 μm in diameter ($PM_{2.5}$) measured by fine dust measuring instrument (Fidas) and aerosol chemical composition measurements by Aerosol Chemical Speciation Monitor (ACSM, Aerodyne Res.), in the immediate proximity of GIF. Note that CO_2 measurements were made at the Integrated Carbon Observation System (ICOS) tall tower in Saclay (SAC, https://icos-atc.lsce.ipsl.fr/panelboard/SAC). The GIF and SAC measurement sites are 2 km apart. We will focus on the winter months in the following analysis. In winter, CO_2 serves as a tracer for soil respiration and combustion processes, CO is a tracer for combustion processes, H_2 is a tracer for soil deposition and traffic emissions (Yver et al., 2009), O_3 is a tracer for surface deposition and chemical removal by nitric oxide (NO, Reis et al. (2000)), $PM_{2.5}$ traces air pollution by fine particles dominated by secondary material and sulfate aerosols (SO_4^{2-}) trace emission/advection of fine particles from coal burning power plants (Petit et al., 2021). ^{222}Rn is a natural radioactive gas emitted by soils and is a good tracer of planetary boundary layer circulation.

2.2.2. *At Trainou (TRN)*

At the TRN tall tower (47.965 N, 2.112 E, https://icos-atc.lsce.ipsl.fr/panelboard/TRN) vertical profiles (5 m and 180 m) of CO_2, CO, and H_2 mixing ratios were monitored with instruments similar to those deployed at the GIF station. The COS vertical distribution was measured using a Quantum Cascade Laser Spectrometer (mini QCLS, Aerodyne Research). The reader is referred to Belviso et al. (2020) for a description of COS measurements using QCLS-Tunable IR Laser Direct Absorption Spectroscopy (TILDAS). ^{222}Rn was measured at a 180 m height by an Australian Nuclear Science and Technology Organisation (ANSTO)-built detector for continuous monitoring of radon concentration in air (Whittlestone and Zahorowski, 1998). At this height, ^{222}Rn is less sensitive to the dynamics of the nocturnal boundary layer and rather traces the transport of air masses over longer distances.

2.2.3. *In the city of Beauvais*

Flask air samples were collected in pairs in May 2019 and March 2020 both upwind and downwind of the largest French emission spot of anthropogenic CS_2 located in Beauvais (49.436 N, 2,07 E), about 80 km NO of Paris city. The sampling device has been described by Lin et al. (2015) and methodological details as well as precision of GC COS measurements of flask-air samples are described in Belviso et al. (2022b). In short, in 90% of the analyses, the difference in COS mixing ratios between flasks of the same pair is less than 14 ppt (Belviso et al., 2022b).

2.3. *Back trajectory calculation*

Back trajectories were calculated following Petit et al. (2017a). With the PC-based version of HYSPLIT (Stein et al., 2015) and using $1° \times 1°$ Global Data Assimilation System (GDAS) files, 120 h back trajectories ending at GIF at 500 m a.g.l. were calculated every 6 h from 2014 to 2020. Calculations using HYSPLIT executables were automatically controlled by ZeFir (Petit et al., 2017b), a user-friendly interface based on Igor Pro 6.3 (Wavemetrics©). The cluster analysis presented in the following was also applied from HYSPLIT executables, controlled by ZeFir. Six clusters were used, in accordance with the total spatial variance (TSV).

3. Results

3.1. *Comparison of Z-2018 to French local emission data*

Fig. 1 shows the spatial distribution of Z-2018 total anthropogenic fluxes of COS for EU27 + UK, France and IDF (Fig. 1A, B and 1C, respectively) for year 2012, annual COS fluxes, in units of Mg S yr^{-1}, being depicted at the top of each panel.

Among the EU27 + UK countries (53943 MgS yr^{-1} in total), Germany appears to be the dominant source region in Europe (15389 Mg S yr^{-1}, i.e., about 29% of total emissions). Poland (6037 Mg S yr^{-1}), Belgium (5362 Mg S yr^{-1}), France (Figs. 1B, 5191 Mg S yr^{-1}), and United Kingdom (4028 Mg S yr^{-1}), are ranked second to fifth, respectively. The IDF region appears to be the most important French hot-spot (Fig. 1B and C), with this region accounting for about 22% of total French emissions (Fig. 1 B, C). Sectorial sources of anthropogenic COS reported as histograms in Fig. S1 for Paris, IDF, France and EU27 + UK, show how their relative contributions differ. The contribution of coal is secondary in France, and even negligible in the case of industrial and residential coal in Paris and IDF. The dominant importance attributed to the rayon sources for France is puzzling because this industry went to decline several decades ago (L.-G. Battentier pers.com. dated 11/28/2018). In France, rayon processors have been substituted by food casings and cellulosic sponge manufacturers, and their CS_2 atmospheric emissions over a 50 t yr^{-1} threshold are subjected to annual declaration. The comparison between data reported in Table 2 and Fig. 1B (for year 2012) show that the Z-2018 inventory does not locate the French CS_2 hotspots correctly and strongly underestimates their COS emissions at least by two orders of magnitude.

Emissions from the sites located in the cities of Beauvais and S^t Hippolyte increased markedly in the early 2010s then reached a plateau, contrary to those of Thaôn-les-Vosges that exhibit a slight decreasing trend since 2012. It is worth noting that the Adisseo Company, a worldwide leader in nutritional solutions and additives for animal feed, which synthetizes and transforms tens of thousands tons of CS_2 into sulfur amino acids from a production unit in les Roches/S^t-Clair-du-Rhône, France (45.4436 N, 4.7646 E), does not meet the IREP reporting criteria of emissions higher than 50 t CS_2 per year.

Direct COS air emissions from coal burning power plants were assessed as by Zumkehr et al. (2018). In general, there is better agreement between Z-2018 and IREP values when CO_2 rather than CS_2 fluxes are used for COS estimates (Table 2). However, the biggest French coal power plant located in Cordemais is misrepresented in the Z-2018 inventory as well as the plant in Vitry-sur-Seine, for which emissions in 2012 appear to be strongly overestimated, i.e., the year of its final closure. In 2020, only two power plants remained operational in France. Nevertheless, as the Cordemais power plant is located in the vicinity of the city of Nantes where Z-2018 COS estimates are equal to 7.7 ± 78.6 pmol m^{-2} s^{-1} (mean ± 1 SD of nine pixels, Fig. 1B, coded Co), one can consider that both inventories agree rather well although for the wrong reasons. Conversely, with coal power plants and viscose processors being absent in IDF, the Z-2018 inventory appears to inadequately represent COS anthropogenic emissions from this area.

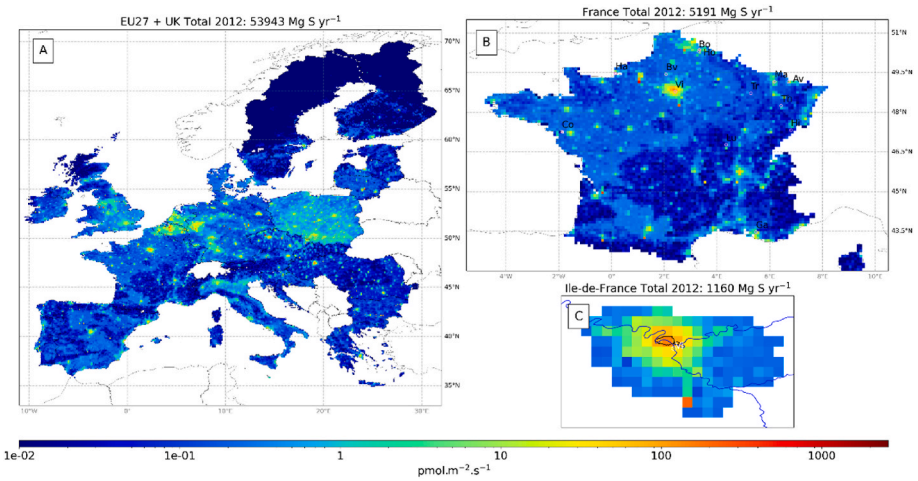

Fig. 1. Plot of the Z-2018 gridded anthropogenic emissions inventory of COS in Europe (A, EU27 + UK), France (B) and the Ile-de-France region (C). Units in pmol m^{-2} s^{-1}. Spatially integrated fluxes are expressed in units of Mg S yr^{-1} depicted at the top of each panel. French declared CS_2 hotspots and coal-burning power plants are letter coded in panel B (see also Table 2).

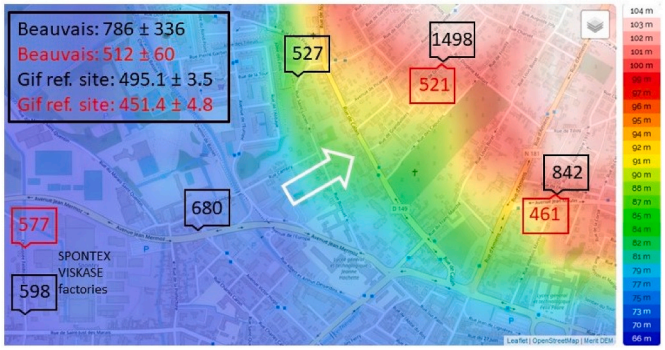

Fig. 2. Averaged COS mixing ratios (units in ppt) measured downwind of the Viskase/Spontex factories overlaid on a topographical map of the city of Beauvais (m a.s.l). Samples were collected May 6th, 2019 (black icons pointing to the sampling location) and March 3rd, 2020 (red icons) when the wind was blowing from the SO (depicted by the central white arrow). A comparison of averaged data gathered simultaneously at Gif and Beauvais is shown in an insert in the upper left corner of this plot (2019 and 2020 data in black and red text, respectively) from which enrichment factors (EF) were calculated. EF are also calculated locally as the maximum COS mole fraction ratio documented in the city of Beauvais.

3.2. Case study of local COS emissions from Beauvais' viscose industry

Direct COS air emissions were indirectly assessed through the measurement of COS enrichment factors (EF) in the city of Beauvais, where the VISKASE and SPONTEX factories stand, and between the Beauvais and GIF sites. In May 2019, atmospheric COS in the city of Beauvais was equal to 786 ± 336 ppt while, at the same time, COS at the GIF site was 495.1 ± 3.5 ppt (Fig. 2, EF = 1.6).

In 2019, the spread of COS variations (assessed as 1 SD mean^{-1}) was approximately 60 times higher in Beauvais than at GIF. This is indicative of local sources of COS present in the area. A maximum EF of 2.8 (i.e., 1498/527 ppt) was recorded at the local scale (Fig. 2). The highest COS levels were recorded on top of a hill downwind of both factories, as the topographical map shows, when the wind was blowing from the SO (Fig. 2). This is consistent with COS being emitted at about 20 m a.g.l. from the factory exhaust fumes, then transported to the furthest sampling places over about 1.4 km. In March 2020, although COS was only 14% richer in Beauvais than at Gif, the spread of measurements still was about 10 times higher at Beauvais than at GIF.

3.3. Cluster analysis of winter COS measurements and back trajectories

3.3.1. Climatology of winter data (2015–2020)

Following Petit et al. (2017a), cluster analysis was applied to HYSPLIT back trajectories calculated every 3 h at the GIF site during the months of December through to March, from 2015 to 2020. Mean trajectories for each cluster are represented in Fig. 3A.

Two clusters out of 6 track continental air-masses exhibiting contrasting COS concentrations. Air masses transported from Scandinavia over Germany, Belgium and northern France (cluster "continental") are significantly richer in COS than those transported from the coast of Britany over central France up to GIF (cluster "anticyclonic", Fig. 3B). The difference between medians of clusters "continental" (i.e., 447 ppt) and "anticyclonic" (i.e., 487 ppt) is 40 ppt, whereas medians of air masses of marine origin or having travelled over the North Atlantic and UK (clusters NW1, NW2, SW and W) are in the range 460–470 ppt.

3.3.2. Selected winter episodes

This cluster analysis of back trajectories applied on winter COS concentrations documented at GIF, was also carried out with higher temporal resolution by focusing on two pollution episodes that took place in January 2016 and February 2018. Pollution advection is illustrated by similar variabilities at the GIF and TRN monitoring stations, which are separated by around 80 km, as shown in Figs. 4 and 5A-D for comparison. The February 2018 time series at the TRN site can be divided in two distinct parts according to the vertical distribution of tracers (Fig. 4).

Several episodes of nocturnal vertical stratification were recorded at TRN before February 20th. They were characterized by CO_2 and CO enhancements (Fig. 4A,B) and H_2 and COS depletions near the ground (Fig. 4C and D). No sign of nocturnal stratification was observed during the second half of the February 2018 record, and the five tracers, including radon measured solely at 180 m (Fig. 4A), exhibited synchronized temporal variations with concentrations culminating on the 21st. Hence, those records suggest that polluted air masses of continental origin were advected over the rural TRN site from February 20th. During that same period, radon, CO_2, CO, H_2 and COS concentrations exhibited similar synchronous variations at GIF than at TRN (Fig. 5A–D), and the transition from nocturnal stratification to vertical mixing took place at GIF (for CO_2, Fig. 5A) almost at the same time as at TRN (Fig. 4).

At GIF, the pollution peak of 21st was associated with high $PM_{2.5}$ and sulfates (Fig. 5C), and low O_3, due to titration of O_3 by NO (Fig. 5D). Among the ground level gas and particle measurements, only sulfate displayed a clear transition from low to high levels, coinciding with the

Table 2
Evaluation using historical French governmental data of Z-2018 gridded inventory of direct/indirect production of COS.

French industrial sources	IREP nb.	Company name/city	Lat.	Long.	2012	2013	2014	2015	2016	2017	2018	2019	2020
Viscose processors[a]	5100918	SPONTEX/**B**eauvais[b]	49.436	2.07	**1408**[c]	2286	3415	3264	4096	3273	3590	2700	3152
	5100909	VISKASE/**B**eauvais			6 ± 6[d]								
	5902583	FACEL/S[t] **Hi**ppolyte	47.324	6.804	**216**	660	502	614	673	656	564	531	394
					8 ± 9								
	6200921	RHOVYL/**Tr**onville-En-Barrois	48.716	5.285	2 ± 1					319	328		
	6202541	VISKASE/**Th**aôn-les-Vosges	48.249	6.43	**2529**	2215	2487	2203	2265	1923	1246	1868	2144
					2 ± 1								
Coal power plants	6301217	**Co**rdemais	47.267	−1.88	**237**[e]	230	128	106	84	188	139	27	31
					2 ± 1								
	6207853	S[t] **Av**old	49.15	6.7	**189**	183	98	140	134	184	119	94	5.2
					43 ± 67								
	6400023	**Ga**rdanne	43.47	5.48	**49**	104	43	75	77	68	13	1.6	
					30 ± 44								
	7000504	**Bo**uchain	50.3	3.31	**34**	32	16	13					
					26 ± 26								
	5802143	Le **Ha**vre	49.47	0.15	**85**	135	19	41	107	93	44	18	22
					12 ± 29								
	7000663	**Ho**rnaing	50.37	3.33	**13**	4							
					24 ± 24								
	5401195	**Lu**cy	46.77	4.35	**16**	15							
					2 ± 1								
	6205633	La **Ma**xe	49.16	6.185	**66**	72	58	27					
					32 ± 29								
	7402281	**Vi**try-sur-Seine	48.78	2.416	**0.7**								
					630 ± 459								

[a] Food casings and cellulosic sponge manufacturers, except Rhovyl a manufacturer of synthetic textile fibers.
[b] Abbreviations in bold are used in Fig. 1.
[c] French governmental data. Units: pmol m^{-2} s^{-1}. 1 tCS_2 yr^{-1} by 0.1° × 0.1° grid cell (i.e., 82.7 km^2 at 48°N) is equivalent to 4.18 pmol m^{-2} s^{-1} as COS assuming a molar yield of 0.83.
[d] Extracted from Z-2018. Mean ± 1SD of 9 pixels of 0.1° × 0.1° each (i.e., the central one + 8 surrounding pixels).
[e] 100,000 tCO_2 yr^{-1} grid $cell^{-1}$ are equivalent to 4.97 pmol m^{-2} s^{-1} as COS assuming a COS/CO_2 molar ratio of 5.7 10^{-6}.

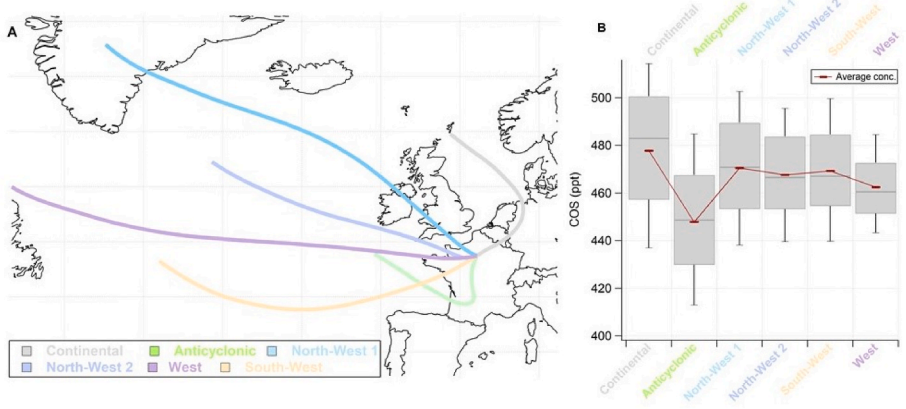

Fig. 3. Mean trajectories for each cluster at the GIF measuring site during winter months (DJFM). The color of each cluster represents its geographical origin (A). Box-plots of COS mixing ratio in GIF's atmosphere sorted by clusters of trajectories (B). The differences in COS concentrations between clusters are significant ($P < 0.002$, Wilcoxon-Mann-Whitney Rank Sum Test, number of data points by cluster: $397 < n < 1094$).

transition from nocturnal stratification to vertical mixing. In other words, there were already signs of air pollution in the suburban atmosphere of GIF before the episode of pollution advection, yet not on the basis of the sulfate record.

A similar multi-tracer approach was applied to a pollution episode that occurred in January 2016 (Fig. 5E–H). There was almost no sign of CO_2 vertical stratification during the two-week period of concern (Fig. 5E). The two broad radon maxima of 2–3 days duration (dated January, 19th-21st and 24th-26th, respectively) and one maximum of shorter duration (dated January, 22nd, Fig. 5E) displayed contrasted levels in terms of mixing ratios and concentrations. The first radon maximum was high in CO_2, CO, H_2, COS, $PM_{2.5}$ and sulfates, and simultaneously low in O_3. That highly resembles the pollution advection episode observed in February 2018. The second broad radon maximum was characterized by CO_2, CO, and $PM_{2.5}$ maxima of smaller intensity than the first, and simultaneously by COS and O_3 minima. The third radon maximum was essentially characterized by its low levels of COS, with all other tracers exhibiting intermediate levels. It is suggested that the second and third radon maxima, which share much in common, would be associated with a local/regional pollution episode of 4–5 days duration that was interrupted on one day (January, 23rd) by advection of cleaner air of marine origin, i.e., richer in COS and O_3, and poorer in Rn, CO_2, CO, PM and sulfates than in continental suburban air.

Clusters of HYSPLIT back trajectories were used to analyze the temporal variability of suspended particles in light of the geographical origins of air masses, following Petit et al. (2017a). In Fig. 6, the origin of

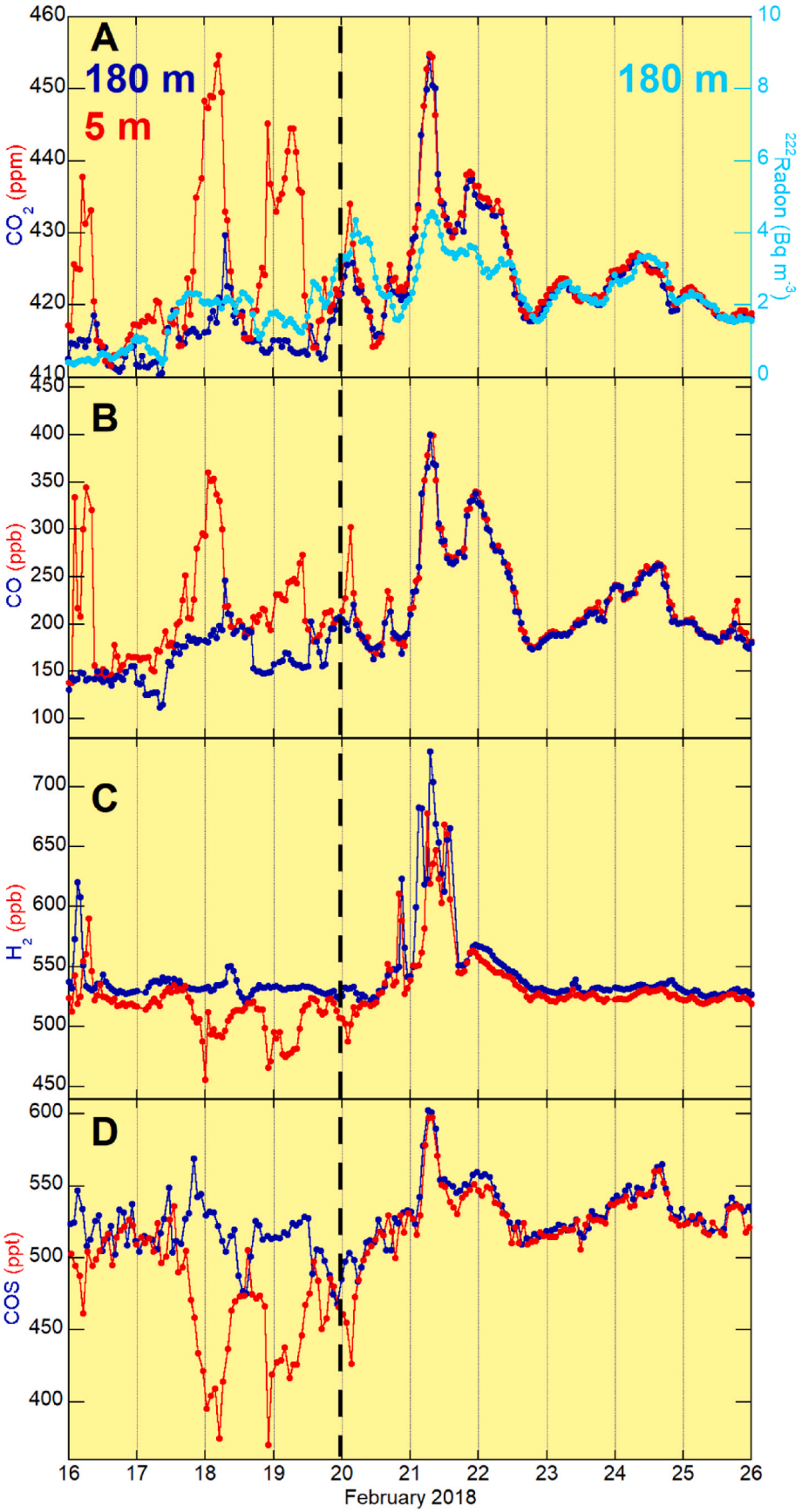

Fig. 4. ^{222}Rn activity and CO_2 mixing ratio (A), CO, H_2 and COS mixing ratios (panels B–D) during February 2018 at TRN. Sampling heights are displayed in panel A. The transition from nocturnal stratification to vertical mixing is depicted as a vertical bold dashed line.

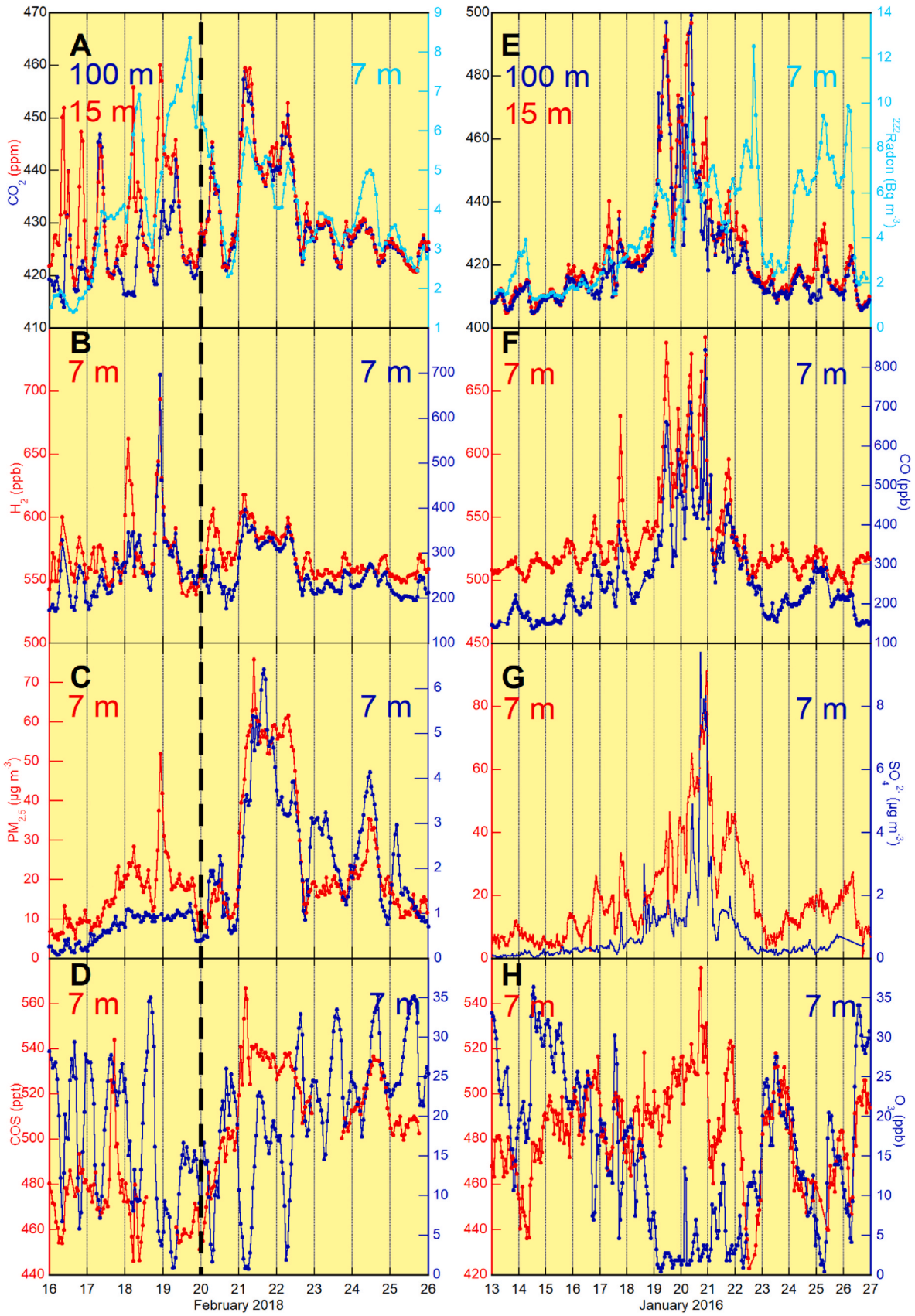

Fig. 5. ^{222}Rn activity and CO_2 mixing ratio (A, B), CO and H_2 mixing ratios (B, F), $PM_{2.5}$ and sulfate concentrations (C, G), and O_3 and COS mixing ratios (D, H) during February 2018 and January 2016 at GIF. Sampling heights are displayed in the top of panels A–D where the transition from nocturnal stratification to vertical mixing is depicted as a vertical bold dashed line according to TRN observations (see Fig. 4).

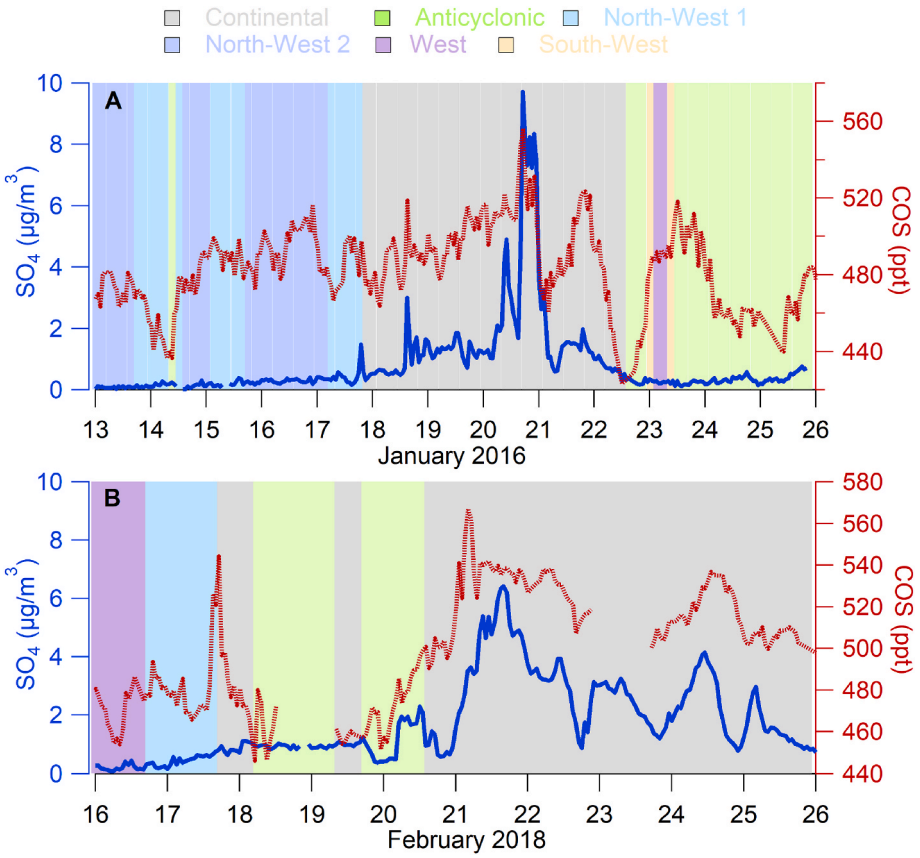

Fig. 6. Temporal variability of sulfates measured by ACSM in GIF in February 2018 (A) and January 2016 (B). Background colors refer to air mass clusters, defined in Fig. 3. COS data is common to this figure and Fig. 5 D,H.

the air mass is illustrated in the background, where each 3-h bin color corresponds to one cluster, as defined in Fig. 3 using the same approach as that illustrated in Fig. 3, yet with a higher temporal resolution.

Clearly, air masses of continental origin (gray background) are richer in sulfates than other air masses. COS and sulfates also exhibit a strong co-variability when air masses are of continental origin.

4. Discussion

Enrichment factors downwind of Beauvais' VISKASE and SPONTEX factories, up to an EF of 2.8 at about a 1.4 km distance from the emission zone, are insufficient if considering food casings and cellulosic sponge manufacturers to be direct emitters of COS. It is thus important to consider the atmospheric transport of CS_2 and its delayed chemical conversion to COS to appropriately represent CS_2 emissions from viscose processors within atmospheric models, i.e., as diffuse rather than point

Table 3
Non exhaustive list of viscose processors in Europe.

Country	City	Company	Product range	latitude	longitude
France	**Be**auvais[a]	Viskase	Artificial casings	49.436	2.07
	Beauvais	Spontex	Sponge cloth		
	Thaôn	Viskase	Artificial casings	48.249	6.43
Germany	**Bo**mlitz	Viskase	Artificial casings	52.905	9.661
	Wiesbaden	Kalle Nalo	Artificial casings	50.033	8.245
	Wiesbaden	Kalle Nalo	Sponge cloth		
	Obernburg	Cordenka	Viscose yarn	49.830	9.148
	Obernburg	Enka	Viscose yarn	49.826	9.147
	Kelheim	Kelheim Fibres	Viscose staple	48.905	11.903
Belgium	**Lo**mmel	Visko Teepak	Artificial casings	51.242	5.254
Finland	**Ha**nko	Visko Teepak	Artificial casings	59.917	23.165
Sweden	**No**rrköping	Freudenberg SE	Sponge cloth	58.592	16.201
Poland	**Kl**eszczow	Sponcel	Sponge cloth	51.269	19.224
Czech Republic	**Lo**vosice	Glanzstoff-Bohemia	Viscose yarn	50.510	14.074
Austria	**Le**nzing	Lenzing AG	Viscose staple	47.979	13.615
Spain	**Ca**seda	Viscofan	Artificial casings	42.547	−1.357
	Malgrat de Mar	Spontex	Sponge cloth	41.644	2.748
	Torrelavega	Sniace	Viscose staple	43.364	−4.052
United Kingdom	**Wi**gton	Futamura chemical	Cellophane	54.828	−3.164

[a] Abbreviations in bold are used in Fig. S2. Courtesy of A. Willers (the VISKASE Group, Germany).

sources of COS (Ma et al., 2021). European production sites of artificial casings are located in France, Germany, Belgium, Finland and Spain (Table 3; A. Willers, Viskase group, pers. com. dated March 18th, 2022).

Those of sponge cloth are located in France, Germany, Sweden, Poland and Spain (Table 3). It is likely that the Z-2018 inventory neglects such major indirect sources of COS, because the use of a sub-country spatial scaling based on industrial N_2O emissions is not suitable for food casings and cellulosic sponge industrial activities. Our assessment based on governmental data also questions the way in which COS emissions estimates have been evaluated in the IDF region. The Vitry-sur-Seine coal power plant was shut down in 2012. Yet estimated emissions from this site are ten to a hundred times higher than those of operational French coal power plants (Table 2). Moreover, because the whole IDF region (2.2% of the inland Metropolitan France) is unrealistically dominated by CS_2 emissions from the rayon industry (Fig. S1B), it accounts for 22.4% of total French COS emissions. Because there are no coal power plants and no rayon industry in the IDF region, it should be essentially considered to be free of anthropogenic COS emissions and the Z-2018 inventory should be revised accordingly. In an attempt to more realistically revise the inventory of CS_2 sources at the European level, we suggest mapping the viscose processing sites listed in Table 3 (see also Fig. S2) and then assigning to each site the average emission rate of the major French food casings and cellulosic sponge manufacturers (VISKASE and SPONTEX), i.e., 610 ± 180 $tCS_2\ yr^{-1}$ for the 2012–2020 period. However, Willers et al. (2013) reported that "biotrickling filters are already used by several companies in the casing industry (four) and one company for the viscose filament and cellophane industry" as a new generation of waste gas treatment techniques. Data collected by EU authorities, available together online at https://eippcb.jrc.ec.europa.eu/sites/default/files/2022-03/WGC_Final_Draft_09Mar2022-B-W-Watermark.pdf, show that 10 out of 11 emission points where more common gas treatment techniques than biotrickling filtration were applied (i.e., regenerative adsorption, CS_2 condensation, thermal or wet catalytic oxidation, scrubbers) exhibited averaged CS_2 molar concentrations in the 20–150 ppm range, including one French site (75 ppm). Biotrickling filtration is expected to reduce CS_2 concentrations at the lower end of that range. Hence, it is expected that French CS_2 emissions to air will follow a decreasing trend in the coming years. As Table 2 shows, this is already the case for direct COS emissions from French coal power plants. In France, titanium oxide is produced by a single plant owned by the Cristal/Tronox company, located in the city of Thann, close to the Swiss and German borders. The plant produces TiO_2 through a sulfate-based process (a wet chemical process that uses sulfuric acid to extract and purify TiO_2 in anatase crystal form) which does not produce COS as a waste non-condensable gas. Only the chloride-based process does so. Hence, the histogram of Fig. S1C does not reflect the reality of French direct and indirect COS emissions. Assuming that COS in France would essentially be released to the atmosphere from coal power plants and viscose processors (Table 2), total COS emissions would have reached 405 Mg S in 2012, i.e., about 8% of Z-2018 estimates. In other words, Z-2018 would overestimate the French COS anthropogenic emissions by about one order of magnitude.

At the European scale, the rayon industry dominates (Fig. S1D), with coal combustion ranking second, on par with the TiO_2 industry. TiO_2 is manufactured in 18 plants in the European Economic Area (EEA, https://rpaltd.co.uk/uploads/report_files/titanium-dioxide-918.pdf, see Tables 3–3 for a map of production facilities in the EEA) yet only a third of these plants use chloride-based process. In that sense, it is concluded that the relative importance of COS emissions from TiO_2 would be overestimated in Europe. Poland accounts for about 50% of EU27 + UK residential and industrial coal emissions, and coal combustion accounts for about 88% of Polish COS emissions (Fig. S3A). Our evaluation of coal emissions from point sources over France (Table 2) tends to support the way in which coal emissions have been represented in the Z-2018 inventory. In the case of Belgium, rayon production accounts for approximately 85% of COS emissions (Fig. S3B), making this country ideal for an evaluation of Z-2018 indirect estimates against governmental data that, unfortunately, is not available yet. The same can apply to Germany where, however, the task would be harder because individual sources exhibit larger diversity than in Poland or Belgium (Fig. S3C).

Remaud et al. (2022) showed that atmospheric COS concentrations simulated by the LMDz atmospheric transport model alongside the Z-2018 inventory, in winter (December to February) during the 2016–2019 period, were overestimated by 100–200 ppt at the GIF site. This is consistent with the IDF region being of secondary importance in the budget of this gas in France. However, the coarse spatial resolution of the LMDz transport model prevents one to go one step further in the assessment of our revised emissions provided in Table 2, because emissions from surrounding countries were not evaluated in the same way. We look forward to perform model simulations based on the FLEXPART Lagrangian particle dispersion model in receptor-oriented mode, which utilizes meteorological data at a 0.2° horizontal resolution.

Baartman et al. (2022) provided a rough first estimate of European COS road traffic emissions of 190 Mg S yr^{-1}, so about half of emissions solely from French viscose processors and coal power plants (i.e., 405 Mg S yr^{-1} in 2012). Baartman's emission flux was estimated from air samples collected in a highway tunnel in the Utrecht region of The Netherlands, which were analyzed for COS and CO_2 mixing ratios, from which a consistent COS/CO_2 enhancement molar ratio of 0.4 10^{-6} was calculated. This ratio is an order of magnitude lower than that used by Z-2018 and ourselves to estimate the COS emissions from coal power plants (Table 2). Hence, it is suggested that assessing CO_2 uptake by plants via COS measurements in European urban areas would not require an accurate knowledge of urban COS sources, provided that cities are free of viscose and coal industrial facilities. However, based on direct eddy covariance COS measurements in Innsbruck (Austria), Karl et al. (2020) suggested that urban COS emissions during August 2018 might be more significant at midday (UTC) on working days (Mondays–Saturdays) than on Sundays, and that vehicular exhausts might be a major COS source in urban areas. We look forward for more direct eddy covariance measurements of COS in the framework of EU funded projects such as the Pilot Application in Urban Landscapes (PAUL). We are also aware that measurements of COS horizontal gradients were carried out in the city of Barcelona in the framework of the EU funded Integrated System Analysis of Urban Vegetation and Agriculture (URBAG). These identified tractable concepts can be used to quantitively re-assess urban COS emissions.

5. Conclusions

Our assessment of the Z-2018 gridded inventory of direct/indirect emissions of COS is based on two complementary approaches: (1) facilities reporting an on-site release to air from France and (2) multi-site observations, near real time data and trajectory analyses that offer a means to target COS emissions of key European countries. We found that the Z-2018 inventory for France largely overestimates COS emissions by about one order of magnitude. We question the use of industrial N_2O to scale CS_2 emissions at the sub-country level in France and instead suggest use of mapped emissions from the viscose processors we identified. The conclusion of our cluster analysis of winter concentrations measured at the GIF site is in agreement with the previous one as to the contrasted role played by France in the European budget of anthropogenic COS. Using the signature of marine air masses as a reference for background air, France is shown to be a net sink of COS whereas Germany and Belgium appear to be net sources. When the cluster analysis is applied at a local scale and with a finer temporal resolution, by targeting two wintertime pollution episodes, COS depletion is associated with local pollution episodes while COS enrichment occurs when air masses are advected up to GIF from the NE sector. Sulfate concentrations are shown to trace the anthropogenic origin of COS from coal-burning power plants. This supports the use by Z-2018 of energy industry SO_2

to scale emissions to the sub-country level in France, although we rather recommend the use of location maps of coal power plants.

CRediT authorship contribution statement

Sauveur Belviso: Conceptualization, Methodology, Validation, Formal analysis, Investigation, Data curation, Writing – original draft, Visualization. **Isabelle Pison:** Methodology, Software, Investigation, Resources, Visualization, Writing – review & editing. **Jean-Eudes Petit:** Methodology, Software, Formal analysis, Investigation, Resources, Data curation, Visualization, Writing – review & editing. **Antoine Berchet:** Methodology, Software, Investigation, Resources, Writing – review & editing. **Marine Remaud:** Writing – review & editing. **Leïla Simon:** Writing – review & editing. **Michel Ramonet:** Funding acquisition, Writing – review & editing. **Marc Delmotte:** Writing – review & editing. **Victor Kazan:** Writing – review & editing. **Camille Yver-Kwok:** Writing – review & editing. **Morgan Lopez:** Writing – review & editing.

Declaration of competing interest

The authors declare that they have no known competing financial interests or personal relationships that could have appeared to influence the work reported in this paper.

Data availability

GIF data is available from https://doi.org/10.14768/6800b065-dcec-4006-ada5-b5f62a4bb832

Acknowledgments

We acknowledge Jim Stinecipher and Elliott Campbell for sharing data and initiating discussions as to the way Z-2018 gridded inventory of direct/indirect emissions of COS could be evaluated at the regional scale.

Appendix A. Supplementary data

Supplementary data to this article can be found online at https://doi.org/10.1016/j.atmosenv.2023.119689.

References

Aydin, M., Britten, G.L., Montzka, S.A., Buizert, C., Primeau, F., Petrenko, V., Battle, M. B., Nicewonger, M.R., Patterson, J., Hmiel, B., Saltzman, E.S., 2020. Anthropogenic impacts on atmospheric carbonyl sulfide since the 19th century inferred from polar firn air and ice core measurements. J. Geophys. Res. Atmos. 125 https://doi.org/10.1029/2020JD033074.

Aydin, M., Williams, M.B., Tatum, C., Saltzman, E.S., 2008. Carbonyl sulfide in air extracted from a South Pole ice core: a 2000 year record. Atmos. Chem. Phys. 8, 7533–7542. https://doi.org/10.5194/acp-8-7533-2008.

Baartman, S.L., Kroll, M.C., Röckmann, T., Hattori, S., Kamesaki, K., Yoshida, N., Popa, M.E., 2022. A GC-IRMS method for measuring sulfur isotope ratios of carbonyl sulfide from small air samples, 2022 Open Research Europe 1, 105. https://doi.org/10.12688/openreseurope.13875-2.

Belviso, S., Abadie, C., Montagne, D., Hadjar, D., Tropée, D., Vialettes, L., Kazan, V., Delmotte, M., Maignan, F., Remaud, M., Ramonet, M., Lopez, M., Yver-Kwok, C., Ciais, P., 2022b. Carbonyl sulfide (COS) emissions in two agroecosystems in central France. PLoS One 17 (12), e0278584. https://doi.org/10.1371/journal.pone.0278584.

Belviso, S., Lebegue, B., Ramonet, M., Kazan, V., Pison, I., Berchet, A., Delmotte, M., Yver-Kwok, C., Montagne, D., Ciais, P., 2020. A top-down approach of sources and non-photosynthetic sinks of carbonyl sulfide from atmospheric measurements over multiple years in the Paris region (France). PLoS One 15, e0228419. https://doi.org/10.1371/journal.pone.0228419.

Belviso, S., Reiter, I.M., Loubet, B., Gros, V., Lathière, J., Montagne, D., Delmotte, M., Ramonet, M., Kalogridis, C., Lebegue, B., Bonnaire, N., Kazan, V., Gauquelin, T., Fernandez, C., Genty, B., 2016. A top-down approach of surface carbonyl sulfide exchange by a Mediterranean oak forest ecosystem in southern France. Atmos. Chem. Phys. 16, 14909–14923. https://doi.org/10.5194/acp-16-14909-2016.

Belviso, S., Remaud, M., Abadie, C., Maignan, F., Ramonet, M., Peylin, P., 2022a. Ongoing decline in the atmospheric COS seasonal cycle amplitude over western Europe: implications for surface fluxes. Atmosphere 13, 812. https://doi.org/10.3390/atmos13050812.

Campbell, J.E., Berry, J.A., Seibt, U., Smith, S.J., Montzka, S.A., Launois, T., Belviso, S., Bopp, L., Laine, M., 2017. Large historical growth in global terrestrial gross primary production. Nature 544, 84–87. https://doi.org/10.1038/nature22030.

Hannigan, J.W., Ortega, I., Shams, S.B., Blumenstock, T., Campbell, J.E., Conway, S., Flood, V., Garcia, O., Griffith, D., Grutter, M., Hase, F., Jeseck, P., Jones, N., Mahieu, E., Makarova, M., Mazière, M., Morino, I., Murata, I., Nagahama, T., Nakijima, H., Notholt, J., Palm, M., Poberovskii, A., Rettinger, M., Robinson, J., Röhling, A.N., Schneider, M., Servais, C., Smale, D., Stremme, W., Strong, K., Sussmann, R., Te, Y., Vigouroux, C., Wizenberg, T., 2022. Global atmospheric OCS trend analysis from 22 NDACC stations. JGR Atmospheres 127. https://doi.org/10.1029/2021JD035764.

Karl, T., Gohm, A., Rotach, M.W., Ward, H.C., Graus, M., Cede, A., Wohlfahrt, G., Hammerle, A., Haid, M., Tiefengraber, M., Lamprecht, C., Vergeiner, J., Kreuter, A., Wagner, J., Staudinger, M., 2020. Studying urban climate and air quality in the Alps: the Innsbruck atmospheric observatory. Bull. Am. Meteorol. Soc. 101, 488–507. https://doi.org/10.1175/BAMS-D-19-0270.1.

Lin, X., Indira, N.K., Ramonet, M., Delmotte, M., Ciais, P., Bhatt, B.C., Reddy, M.V., Angchuk, D., Balakrishnan, S., Jorphail, S., Dorjai, T., Mahey, T.T., Patnaik, S., Begum, M., Brenninkmeijer, C., Durairaj, S., Kirubagaran, R., Schmidt, M., Swathi, P. S., Vinithkumar, N.V., Yver Kwok, C., Gaur, V.K., 2015. Long-lived atmospheric trace gases measurements in flask samples from three stations in India. Atmos. Chem. Phys. 15, 9819–9849. https://doi.org/10.5194/acp-15-9819-2015.

Ma, J., Kooijmans, L.M.J., Cho, A., Montzka, S.A., Glatthor, N., Worden, J.R., Kuai, L., Atlas, E.L., Krol, M.C., 2021. Inverse modelling of carbonyl sulfide: implementation, evaluation and implications for the global budget. Atmos. Chem. Phys. 21, 3507–3529. https://doi.org/10.5194/acp-21-3507-2021.

Montzka, S.A., Aydin, M., Battle, M., Butler, J.H., Saltzman, E.S., Hall, B.D., Clarke, A.D., Mondeel, D., Elkins, J.W., 2004. A 350-year atmospheric history for carbonyl sulfide inferred from Antarctic firn air and air trapped in ice. J. Geophys. Res. 109, D22302 https://doi.org/10.1029/2004JD004686.

Montzka, S.A., Calvert, P., Hall, B.D., Elkins, J.W., Conway, T.J., Tans, P.P., Sweeney, C., 2007. On the global distribution, seasonality, and budget of atmospheric carbonyl sulfide (COS) and some similarities to CO_2. J. Geophys. Res. 112, D09302 https://doi.org/10.1029/2006JD007665.

Petit, J.-E., Amodeo, T., Meleux, F., Bessagnet, B., Menut, L., Grenier, D., Pellan, Y., Ockler, A., Rocq, B., Gros, V., Sciare, J., Favez, O., 2017a. Characterising an intense PM pollution episode in March 2015 in France from multi-site approach and near real time data: climatology, variabilities, geographical origins and model evaluation. Atmos. Environ. 155, 68–84. https://doi.org/10.1016/j.atmosenv.2017.02.012.

Petit, J.-E., Favez, O., Albinet, A., Canonaco, F., 2017b. A user-friendly tool for comprehensive evaluation of the geographical origins of atmospheric pollution: wind and trajectory analyses. Environ. Model. Software 88, 183–187. https://doi.org/10.1016/j.envsoft.2016.11.022.

Petit, J.-E., Dupont, J.-C., Favez, O., Gros, V., Zhang, Y., Sciare, J., Simon, L., Truong, F., Bonnaire, N., Amodeo, T., Vautard, R., Haeffelin, M., 2021. Response of atmospheric composition to COVID-19 lockdown measures during spring in the Paris region (France). Atmos. Chem. Phys. 21, 17167–17183. https://doi.org/10.5194/acp-21-17167-2021.

Reis, S., Simpson, D., Friedrich, R., Jonson, J.E., Unger, S., Obermeier, A., 2000. Road traffic emissions – predictions of future contributions to regional ozone levels in Europe. Atmos. Environ. 34, 4701–4710. https://doi.org/10.1016/S1352-2310(00)00202-8.

Remaud, M., Chevallier, F., Maignan, F., Belviso, S., Berchet, A., Parouffe, A., Abadie, C., Bacour, C., Lennartz, S., Peylin, P., 2022. Plant gross primary production, plant respiration and carbonyl sulfide emissions over the globe inferred by atmospheric inverse modelling. Atmos. Chem. Phys. 22, 2525–2552. https://doi.org/10.5194/acp-22-2525-2022.

Stein, A.F., Draxler, R.R., Rolph, G.D., Stunder, B.J.B., Cohen, M.D., Ngan, F., 2015. NOAA's HYSPLIT atmospheric transport and dispersion modeling system. Bull. Am. Meteorol. Soc. 96, 2059–2077. https://doi.org/10.1175/BAMS-D-14-00110.1.

Whelan, M.E., Lennartz, S.T., Gimeno, T.E., Wehr, R., Wohlfahrt, G., Wang, Y., Kooijmans, L.M.J., Hilton, T.W., Belviso, S., Peylin, P., Commane, R., Sun, W., Chen, H., Kuai, L., Mammarella, I., Maseyk, K., Berkelhammer, M., Li, K.-F., Yakir, D., Zumkehr, A., Katayama, Y., Ogée, J., Spielmann, F.M., Kitz, F., Rastogi, B., Kesselmeier, J., Marshall, J., Erkkilä, K.-M., Wingate, L., Meredith, L.K., He, W., Bunk, R., Launois, T., Vesala, T., Schmidt, J.A., Fichot, C.G., Seibt, U., Saleska, S., Saltzman, E.S., Montzka, S.A., Berry, J.A., Campbell, J.E., 2018. Reviews and syntheses: carbonyl sulfide as a multi-scale tracer for carbon and water cycles. Biogeosciences 15, 3625–3657. https://doi.org/10.5194/bg-15-3625-2018.

Whittlestone, S., Zahorowski, W., 1998. Baseline radon detectors for shipboard use: development and deployment in the first aerosol characterization experiment (ACE 1). J. Geophys. Res. 103, 16743–16751. https://doi.org/10.1029/98JD00687.

Willers, A., Dressler, C., Kennes, C., 2013. Biotrickling filtration of waste gases from the viscose industry. In: Kennes, C., Veiga, M.C. (Eds.), Air Pollution Prevention and Control. John Wiley & Sons, Ltd, Chichester, UK, pp. 465–484. https://doi.org/10.1002/9781118523360.ch19.

Yan, Y., Li, R., Peng, L., Yang, C., Liu, C., Cao, J., Yang, F., Li, Y., Wu, J., 2019. Emission inventory of carbonyl sulfide (COS) from primary anthropogenic sources in China. Environ. Pollut. 247, 745–751. https://doi.org/10.1016/j.envpol.2019.01.096.

Yver, C., Schmidt, M., Bousquet, P., Zahorowski, W., Ramonet, M., 2009. Estimation of the molecular hydrogen soil uptake and traffic emissions at a suburban site near Paris through hydrogen, carbon monoxide, and radon-222 semicontinuous measurements. J. Geophys. Res. 114, D18304 https://doi.org/10.1029/2009JD012122.

Zumkehr, A., Hilton, T.W., Whelan, M., Smith, S., Kuai, L., Worden, J., Campbell, J.E., 2018. Global gridded anthropogenic emissions inventory of carbonyl sulfide. Atmos. Environ. 183, 11–19. https://doi.org/10.1016/j.atmosenv.2018.03.063.